

Transmission of a Phononic Superlattice Made of Dynamic Materials

S. GARUS^{a,*}, W. SOCHACKI^a, J. GARUS^a,
J. RZĄCKI^b, P. VIZUREANU^{c,d} AND A.V. SANDU^{c,e,f}

^a*Department of Mechanics and Fundamentals of Machinery Design, Faculty of Mechanical Engineering and Computer Science, Czestochowa University of Technology, Dąbrowskiego 73, 42-201 Czestochowa, Poland*

^b*Department of Physics, Faculty of Production Engineering and Materials Technology, Czestochowa University of Technology, Dąbrowskiego 73, 42-201 Czestochowa, Poland*

^c*Faculty of Materials Science and Engineering, Gheorghe Asachi Technical University of Iasi, Blvd. D. Mangeron 71, 700050, Iasi, Romania*

^d*Technical Sciences Academy of Romania, Dacia Blvd 26, 030167 Bucharest, Romania*

^e*Romanian Inventors Forum, Str. Sf. P. Movila 3, 700089 Iasi, Romania*

^f*Academy of Romanian Scientists, 54 Splaiul Independentei St., Sect. 5, 050094, Bucharest, Romania*

Doi: [10.12693/APhysPolA.144.317](https://doi.org/10.12693/APhysPolA.144.317)

*e-mail: sebastian.garus@pcz.pl

In one-dimensional phononic crystals, as a result of multiple destructive interferences of a mechanical wave, the phononic band gap phenomenon occurs, i.e., the lack of propagation of a wave of a given frequency through the structure due to internal reflections at the layer boundary and destructive interference. In dynamic phononic crystals, the incident monochromatic mechanical wave at the boundary of the media does not propagate according to Fresnel's relations, but is transformed into a wave spectrum, which affects the phononic properties of the examined structures and allows them to be dynamically controlled. The paper analyzes the transmission and influence of the frequency of changes in the properties of the elements of the finite phononic structure described by sinusoidal functions on the propagation of mechanical waves.

topics: bandgap, finite-difference time-domain (FDTD), discrete Fourier transform (DFT), superlattice

1. Introduction

The first works on wave propagation in phononic crystals were written at the end of the 19th century. Initial considerations concerned static periodic structures. These structures exhibit unique dynamic properties, thanks to which they act as mechanical wave propagation filters only for specific material solids and geometries. It is in such structures that the so-called band gaps are created, i.e., frequency bands for which waves do not pass through a given structure. Among the many literature items describing this issue in various contexts, one can mention works such as [1–8].

Other structures that have been studied for many decades are quasi-static structures. In these structures, a specific parameter is changed and the properties of the phononic crystal are measured again. Works in this field include, for example, [9–13].

Controlling periodic phononic structures is a more complex issue and concerns the so-called dynamic phononic crystals. The work [14] presents the control of wave propagation in order to stop or limit the propagation of undesirable disturbances resulting from vibrations of the tested structure. A proposal to dynamically change the behavior of phononic crystals by changing material parameters as a function of time is presented in [15]. An interesting study on the propagation of time-varying parameters for phononic crystals was performed in [16] and [17]. The analysis of the time-varying Bragg reflector was presented by the authors in [18].

One way to determine the influence of time-varying material parameters is to use the finite-difference time-domain (FDTD) method, which is a common and versatile approach to acoustic simulation [19] and a starting point for the analysis of time-varying phononic crystals [20].

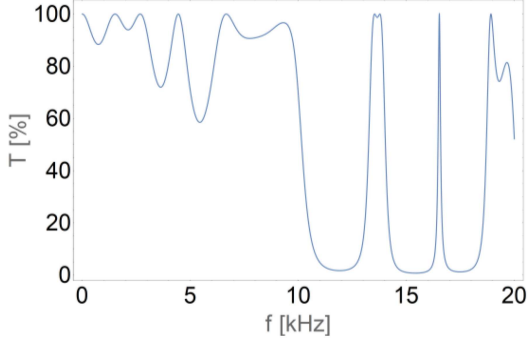


Fig. 1. Transmission of mechanical waves for a static Severin structure.

TABLE I

Material parameters used for calculations for the static phononic structure for the environment and layer A (water) [21] and for layer B (PLA) [22].

Layer	c [m/s]	ρ [kg/m ³]	Z ($\times 10^6$) [kg/(s m ²)]
A (water)	1480	1000	1.48
B (PLA)	2220	1240	2.7528

In this work, the influence of dynamic material coefficients on the propagation and transmission of a mechanical wave inside the aperiodic quasi-one-dimensional Severin structure is analyzed.

2. Research

The propagation of a mechanical wave in a fifth-generation aperiodic Severin superlattice with a $(AB)_2B_2(AB)_3B_2(AB)_3AB_3(AB)_3B_2AB$ layer distribution was analyzed. The subscript indicates the number of repetitions of a given layer or (in brackets) a group of layers. The material parameters of the analyzed layers are summarized in Table I. The assumed thickness of each layer was 0.02 m, and the structure was immersed in water.

In order to determine the frequency values for which the phononic band gap occurs (no propagation of a wave of a given frequency in the structure due to the interference of a destructive mechanical wave occurring inside the phononic crystal) and the frequency for the high transmission band, the transfer matrix algorithm presented in [23] was used. Figure 1 shows the obtained transmission distribution for the analyzed Severin structure.

As shown in [23], in the transmission structure there is a high transmission peak with a small half-width for the propagating wave frequency of 16529 Hz surrounded by bandgap areas.

In order to analyze the mechanical wave propagation in the dynamic aperiodic Severin structure, the finite-difference time-domain (FDTD) algorithm was used, in which the mechanical wave propagation is described by

$$\begin{cases} \frac{\partial P(x,y,z,t)}{\partial t} = Z(t) c(t) \nabla \cdot \mathbf{v}(x,y,z,t), \\ \frac{Z(t)}{c(t)} \frac{\partial \mathbf{v}(x,y,z,t)}{\partial t} = \nabla P(x,y,z,t), \end{cases} \quad (1)$$

where $P(x,y,z,t)$ is the pressure field described in three-dimensional space (x,y,z) and at time t , $\mathbf{v}(x,y,z,t)$ is the vector velocity field. The material properties are described by time-dependent functions of the acoustic impedance $Z(t)$ and the phase velocity $c(t)$.

In the formalism of the FDTD method, taking into account the dynamic properties of the material, the system of equations (1) for the quasi-one-dimensional case can be written as

$$\begin{cases} P_k^{n+\frac{1}{2}} = P_k^{n-\frac{1}{2}} + \frac{\Delta t Z_k(t) c_k(t) [v_{k+\frac{1}{2}}^n - v_{k-\frac{1}{2}}^n]}{\Delta z} \\ v_{k+\frac{1}{2}}^{n+1} = v_{k+\frac{1}{2}}^n + \frac{\Delta t c_k(t) [P_{k+1}^{n+\frac{1}{2}} - P_k^{n+\frac{1}{2}}]}{\Delta z Z_k(t)} \end{cases} \quad (2)$$

Here, Δz and Δt define steps in space and time, respectively, and to ensure the stability of the simulation they must satisfy the Courant stability condition $\Delta t \leq \Delta z/c_{\max}$, where c_{\max} means the highest possible phase velocity of a propagating mechanical wave. In (2), k is the spatial step number. In this work, PML boundary conditions were used to extinguish the wave going beyond the examined area. A soft mechanical wave source with a frequency f_S was used

$$\begin{cases} Z_n(t) = Z_{n,0} + \frac{D_n}{2} Z_{n,0} \sin(2\pi f_n t) \\ c_n(t) = c_{n,0} + \frac{D_n}{2} c_{n,0} \sin(2\pi f_n t) \end{cases} \quad (3)$$

where n corresponds to a given type of material in the layer (A or B), $Z_{n,0}$ and $c_{n,0}$ are the acoustic impedance and phase velocity of the material in the layer n , respectively, and D_n is percentage change in the amplitude of the variable component of material parameters.

In the first analyzed case, a ten percent change in the amplitude of material values ($D_A = D_B = 10\%$) was assumed with a frequency equal to the frequency of the wave source ($f_S = f_A = f_B = 16529$ Hz) for high transmission peak. Using the FDTD and discrete Fourier transform (DFT) algorithms, the distribution of local resonance fields was determined (Fig. 2). Figure 3 shows the spatial distribution of local resonance areas that occurred at the frequency of 8375 Hz. Vertical or horizontal lines in the graphs, respectively, indicate layer boundaries.

The shift in the frequency of the local resonance areas from the source frequency of 16529 Hz to the frequency of 8375 Hz compared to the static structure [23] and the significant increase in the amplitude of the mechanical wave in the analyzed areas is caused by the resonance occurring due to the correspondence of the vibrations of the medium and the source.

In the second case (Fig. 4 and Fig. 5), only the time-varying values of the material parameters of layers B were analyzed with a frequency consistent

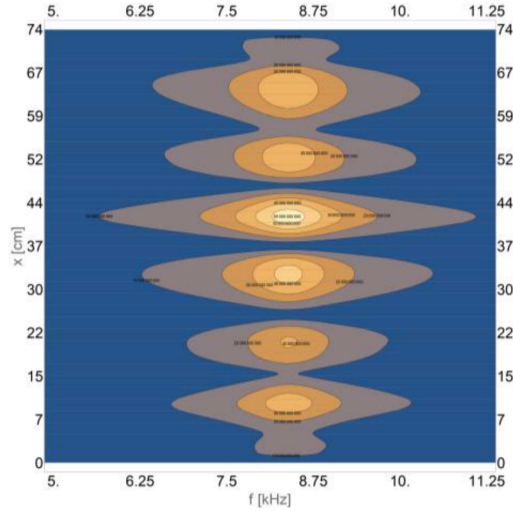


Fig. 2. Distribution of local resonance fields for the source frequency equal to $f_S=16529$ Hz for materials values pulsating with the frequency of the source with the vibration amplitude equal to 10% of the mediums parameters.

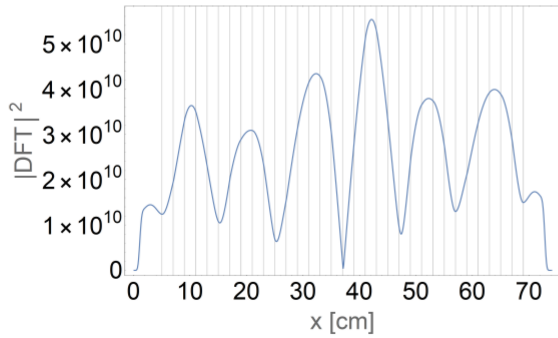


Fig. 3. Spatial distribution of local resonance areas that occurred at the frequency of 8375 Hz in the case of $D_A=D_B=10\%$ and $f_S=f_A=f_B=16529$ Hz.

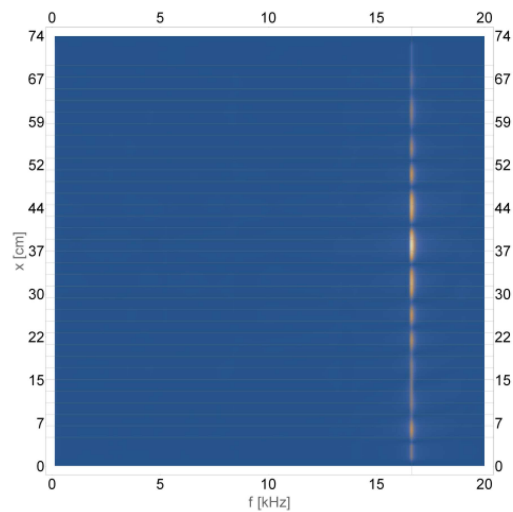


Fig. 4. Distribution of local resonance fields for $f_S = f_B = 16529$ Hz, $f_A = 0$ Hz, $D_A = 0$, and $D_B = 10\%$.

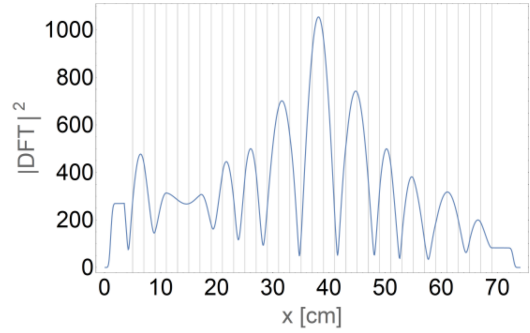


Fig. 5. Spatial distribution of local resonance areas that occurred at the frequency of 16529 Hz in the case of $f_S = f_B = 16529$ Hz, $f_A = 0$ Hz, $D_A = 0$, and $D_B = 10\%$.

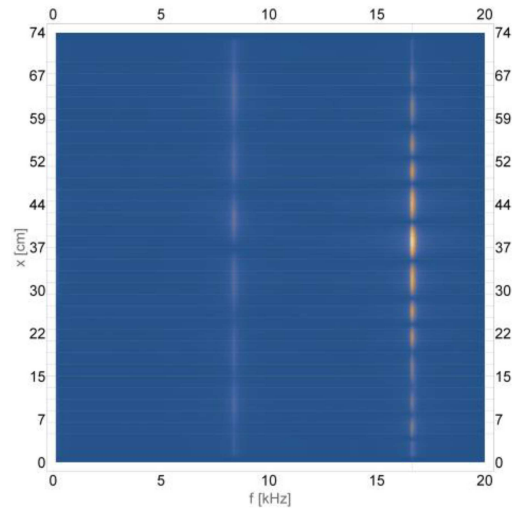


Fig. 6. Distribution of local resonance fields for $f_S = f_B = 16529$ Hz, $f_A = 0$ Hz, $D_A = 0$, and $D_B = 12\%$.

with the frequency of the mechanical wave source ($f_S = f_B = 16529$ Hz, $f_A = 0$), where the amplitude change was 10% ($D_A = 0$, $D_B = 10\%$). Compared to a structure made of materials with static properties [23], the value of the amplitude of mechanical vibrations in local resonance areas was reduced by two times. By increasing the value of the amplitude change to $D_B = 12\%$ (Fig. 6 and Fig. 7), an additional frequency was observed in the spectrum, which corresponded to the value from the first analyzed case in which resonance was observed.

In the last analyzed case (Fig. 8 and Fig. 9), the oscillation frequency of material B was reduced in relation to the source frequency by 10% ($f_B = 90\%$, $f_S = 14876$ Hz, $f_A = 0$ Hz), with the amplitude of changes in the values of material parameters equal to 10% ($D_A = 0$, $D_B = 10\%$).

Apart from the source frequency, two additional frequencies were also observed in the spectrum, i.e., 13375 Hz and 1750 Hz, for which there were local resonance areas within the analyzed phononic structure.

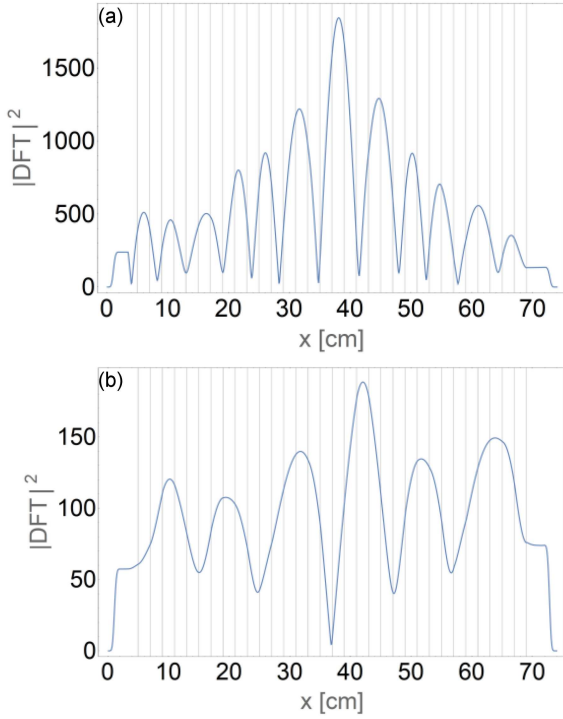


Fig. 7. Spatial distribution of local resonance areas in the case of $f_S = f_B = 16529$ Hz, $f_A = 0$ Hz, $D_A = 0$, and $D_B = 12\%$, which occurred at frequencies (a) 16529 Hz and (b) 8375 Hz.

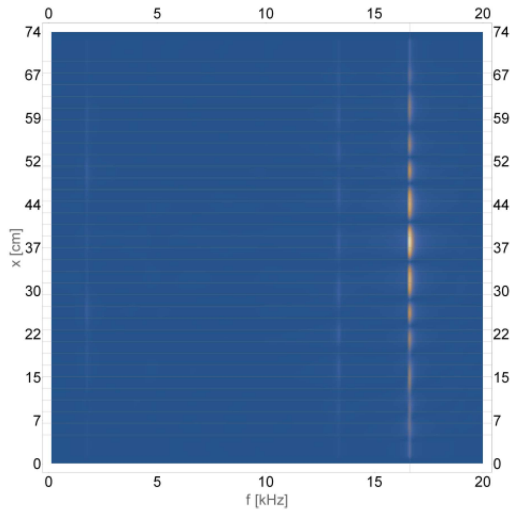


Fig. 8. Distribution of local resonance fields for $f_B = 90\%$, $f_S = 14876$ Hz, $f_A = 0$ Hz, $D_A = 0$, and $D_B = 10\%$.

3. Conclusions

The tests carried out showed the existence of band gaps in the transmission spectrum for the Severin aperiodic phononic structure. The introduction of vibrations in the values of material parameters (acoustic impedance and density) for all simulation

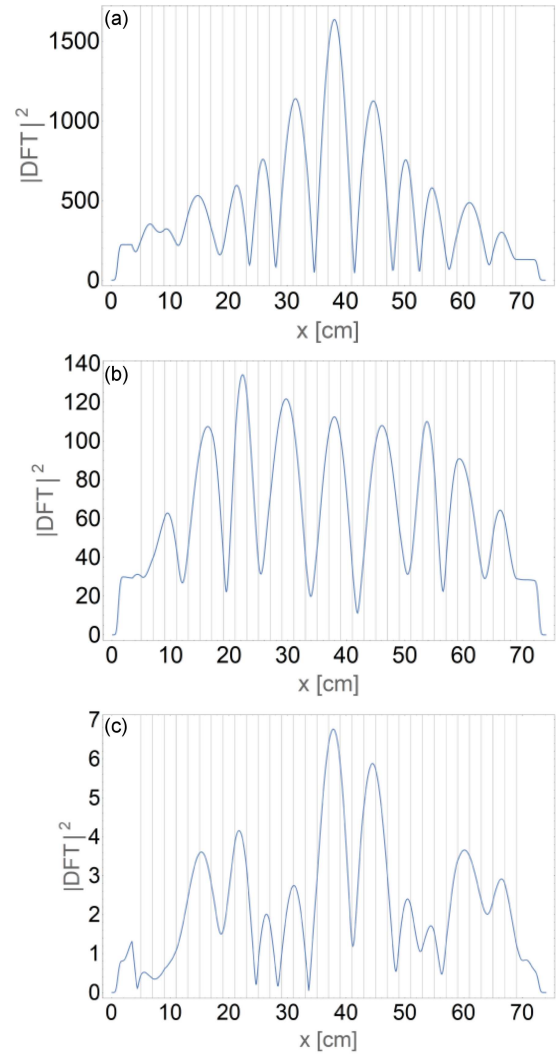


Fig. 9. Spatial distribution of local resonance areas in the case of $f_B = 90\%$, $f_S = 14876$ Hz, $f_A = 0$ Hz, $D_A = 0$, and $D_B = 10\%$, which occurred at frequencies (a) 16529 Hz, (b) 13375 Hz, and (c) 1750 Hz.

materials with a frequency equal to the frequency of the wave source caused the phenomenon of resonance and a shift of the transmission peak towards lower frequencies, reducing the number of local resonance areas and increasing the amplitude of the mechanical wave propagating in the material. The introduction of 10% changes in the vibration amplitudes of the acoustic impedance and the density of only the B material resulted in a reduction of the amplitude and energy of the mechanical wave in local resonance areas and changed their distribution. Another increase in the amplitude by 2% resulted in the creation of an additional local resonance region at the frequency of 8.3 kHz. For the vibration frequency of parameters of the material B equal to 90% of the source vibration frequency, there were 3 groups of local resonance areas: 1.6 kHz, 13.3 kHz, and 16.6 kHz.

References

- [1] X.-F. Li, X. Ni, L. Feng, M.-H. Lu, C. He, Y.-F. Chen, *Phys. Rev. Lett.* **106**, 084301 (2011).
- [2] R. Martínez-Sala, J. Sancho, J.V. Sánchez, V. Gómez, J. Llinares, F. Meseguer, *Nature* **378**, 241 (1995).
- [3] M.S. Kushwaha, P. Halevi, L. Dobrzyński, B. Djafari-Rouhani, *Phys. Rev. Lett.* **71**, 2022 (1993).
- [4] S. Garus, W. Sochacki, *J. Appl. Math. Comput. Mech.* **16**, 17 (2017).
- [5] A. Sukhovich, L. Jing, J.H. Page, *Phys. Rev. B* **77**, 014301 (2008).
- [6] Jin-Chen Hsu, Tsung-Tsong Wu, *IEEE Trans. Ultrason. Ferroelectr. Freq. Control* **53**, 1169 (2006).
- [7] S. Garus, W. Sochacki, M. Bold, *Eng. Mech.* **2018**, 229 (2018).
- [8] G. Wang, X. Wen, J. Wen, L. Shao, Y. Liu, *Phys. Rev. Lett.* **93**, 154302 (2004).
- [9] X. Li, F. Wu, H. Hu, S. Zhong, Y. Liu, *J. Phys. D Appl. Phys.* **36**, L15 (2003).
- [10] W-P. Yang, L-W. Chen, *Smart Mater. Struct.* **17**, 015011 (2008).
- [11] M. Ruzzene, A. Baz, *J. Vib. Acoust.* **122**, 151 (2000).
- [12] O. Thorp, M. Ruzzene, A. Baz, *Smart Mater. Struct.* **10**, 979 (2001).
- [13] A. Singh, D.J. Pines, A. Baz, *Smart Mater. Struct.* **13**, 689 (2004).
- [14] A. Baz, *J. Vib. Acoust.* **123**, 472 (2001).
- [15] D.W. Wright, R.S.C. Cobbold, *Smart Mater. Struct.* **18**, 015008 (2009).
- [16] E.S. Cassedy, *Proc. IEEE* **55**, 1154 (1967).
- [17] C. Elachi, *IEEE Trans. Antennas Propag.* **20**, 534 (1972).
- [18] J.H. Wu, T.H. Cheng, A.Q. Liu, *Appl. Phys. Lett.* **89**, 263103 (2006).
- [19] Y. Tanaka, Y. Tomoyasu, S-I. Tamura, *Phys. Rev. B* **62**, 7387 (2000).
- [20] X. Liu, D.A. McNamara, *Int. J. Infrared Milli. Waves* **28**, 759 (2007).
- [22] Y. Wang, W. Song, E. Sun, R. Zhang, W. Cao, *Physica E* **60**, 37 (2014).
- [23] D. Tarrazó-Serrano, S. Castiñeira-Ibáñez, E. Sánchez-Aparisi, A. Uris, C. Rubio, *Appl. Sci.* **8**, 2634 (2018).
- [24] S. Garus, W. Sochacki, J. Garus, J. Rzącki, *Acta Phys. Pol. A* **142**, 7 (2022).